

Mixing and CPV in the B_d and B_s systems at ATLAS

Evelina Bouhova-Thacker^{*†}

Lancaster University

E-mail: e.bouhova@cern.ch

The most recent results on mixing and CP violation in the B^0 and B_s^0 systems published by the ATLAS experiment at the LHC are presented. The measurement of the $B_s^0 \rightarrow J/\psi\phi$ decay parameters, using data collected in pp collisions at $\sqrt{s} = 7$ TeV and $\sqrt{s} = 8$ TeV and corresponding to 4.9 fb^{-1} and 14.3 fb^{-1} of integrated luminosity, includes the CP -violating phase ϕ_s and the width difference of the mass eigenstates $\Delta\Gamma_s$. The combined Run-1 results are $\phi_s = (-0.098 \pm 0.084(\text{stat.}) \pm 0.040(\text{syst.}))$ rad and $\Delta\Gamma_s = (0.083 \pm 0.011(\text{stat.}) \pm 0.007(\text{syst.})) \text{ ps}^{-1}$. The measured values agree with the Standard Model predictions. The second result presented is the measurement of the relative width difference $\Delta\Gamma_d/\Gamma_d$ of the $B^0-\bar{B}^0$ system, using data collected in pp collisions at $\sqrt{s} = 7$ TeV and $\sqrt{s} = 8$ TeV, and corresponding to a total integrated luminosity of 25.2 fb^{-1} . The measured value is $\Delta\Gamma_d/\Gamma_d = (-0.1 \pm 1.1 (\text{stat.}) \pm 0.9 (\text{syst.})) \times 10^{-2}$. Currently, this is the most precise single measurement of $\Delta\Gamma_d/\Gamma_d$. It agrees with the Standard Model prediction and measurements by other experiments.

XIII International Conference on Heavy Quarks and Leptons

22- 27 May, 2016

Blacksburg, Virginia, USA

^{*}Speaker.

[†]On behalf of the ATLAS Collaboration.

1. The ATLAS detector

The ATLAS experiment uses a general-purpose detector consisting of an inner tracker, electromagnetic and hadronic calorimeters and a muon spectrometer [1]. The analyses presented here use information from the inner detector and the muon spectrometer. The muon spectrometer provides muon identification and triggers. The inner detector provides momentum measurements in the pseudorapidity range $|\eta| < 2.5$. The ATLAS trigger system employs a Level-1 hardware trigger and two high-level software triggers. The analyses use trigger selections based on a di-muon signature. These triggers have muon transverse momentum (p_T) thresholds of 4 or 6 GeV and pseudorapidity coverage of $|\eta| < 2.4$.

2. CP violation in the $B_s^0 \rightarrow J/\psi\phi$ decay

The CP violating weak phase ϕ_s in $B_s^0 \rightarrow J/\psi\phi$ decays is the weak phase difference between the $b \rightarrow c\bar{c}s$ decay amplitude and the $B_s^0 - \bar{B}_s^0$ mixing amplitude. In the Standard Model (SM), ϕ_s is predicted to be small [2]:

$$\phi_s \approx -2\beta_s = 2\arg\left(-\frac{V_{ts}V_{tb}^*}{V_{cs}V_{cb}^*}\right) = -0.0363_{-0.0015}^{+0.0016} \text{ rad} \quad (2.1)$$

and has attracted a lot of interest due to possible new physics contributions to this decay mode:

$$\phi_s = \phi_s^{SM} + \phi_s^{NP}. \quad (2.2)$$

Precise measurements of ϕ_s performed by the LHC experiments have considerably reduced the possible amount of new physics contribution but higher precision is still needed for a stringent test of the SM and to evaluate ϕ_s^{NP} . The value of the width difference of the B_s^0 mass eigenstates $\Delta\Gamma_s$ is predicted to be $\Delta\Gamma_s = (0.087 \pm 0.021) \text{ ps}^{-1}$ [3].

The results of the $B_s^0 \rightarrow J/\psi\phi$ analysis, using 4.9 fb^{-1} of integrated luminosity collected by ATLAS in 2011 at $\sqrt{s} = 7 \text{ TeV}$, were published in 2014 [4]. The measured values are:

$$\phi_s = (0.12 \pm 0.25 \text{ (stat.)} \pm 0.05 \text{ (syst.)}) \text{ rad}, \quad (2.3)$$

$$\Delta\Gamma_s = (0.053 \pm 0.021 \text{ (stat.)} \pm 0.010 \text{ (syst.)}) \text{ ps}^{-1}. \quad (2.4)$$

The analysis of 14.3 fb^{-1} of integrated luminosity collected in 2012 at $\sqrt{s} = 8 \text{ TeV}$, in addition to the increased data sample, includes a number of improvements over the 2011 analysis. The values of the physical parameters measured with 14.3 fb^{-1} of 8 TeV data were statistically combined with those measured with the 4.9 fb^{-1} of 7 TeV data and published in [5]. A brief description of the analysis with 14.3 fb^{-1} at $\sqrt{s} = 8 \text{ TeV}$ and of the Run-1 combination follows.

The $B_s^0 \rightarrow J/\psi\phi$ candidates are selected by fitting four track combinations (two muon tracks and two hadronic tracks) to a common vertex. A J/ψ -mass constraint is applied in the fit. The muon tracks are required to pass the trigger thresholds of $p_T > 4$ or 6 GeV and $|\eta| < 2.4$. The hadronic tracks are required to be oppositely charged and have $p_T > 1 \text{ GeV}$ and $|\eta| < 2.5$. All selection criteria are independent of the B_s^0 lifetime. A total of $375987 B_s^0$ candidates are selected with

$5.15 < m(J/\psi\phi) < 5.65$ GeV. The number of signal candidates is $\approx 75\text{k}$, which is approximately 3.5 times that of the sample used in the 2011 analysis.

The initial flavour of the B_s^0 meson is determined by the flavour of the accompanying B meson. The flavour tagging algorithm is calibrated using self-tagging $B^\pm \rightarrow J/\psi K^\pm$ events from data. Three flavour tagging methods are used: muon, electron and jet charge tagging. The jet charge tag uses the jet with the highest value of b -tag weight in the event, excluding the jet containing the B_s^0 decay. The tagging variable is given by:

$$Q = \frac{\sum_i q^i (p_T^i)^k}{\sum_i (p_T^i)^k}, \quad (2.5)$$

where q^i and p_T^i are the charge and transverse momentum of track i . For muon (electron) tagging, $k = 1.1$ (1.0) and the sum is over tracks within a cone of $\Delta R < 0.5$ around the muon (electron). For jet charge tagging, $k = 1.1$ and the sum is over all tracks in the jet.

An unbinned maximum likelihood fit is used to extract the values of the physical parameters of the $B_s^0 \rightarrow J/\psi\phi$ decay. The information used by the fit includes several variables describing the $B_s^0 \rightarrow J/\psi\phi$ decay: the reconstructed mass, transverse momentum, proper decay length and its uncertainty, angles describing the kinematics of the B_s^0 decay and the flavour tagging probability value. The maximum likelihood fit of the 8 TeV data sample yields the following results:

$$\phi_s = (-0.123 \pm 0.089 \text{ (stat.)} \pm 0.041 \text{ (syst.)}) \text{ rad}, \quad (2.6)$$

$$\Delta\Gamma_s = (0.096 \pm 0.013 \text{ (stat.)} \pm 0.007 \text{ (syst.)}) \text{ ps}^{-1}. \quad (2.7)$$

Figure 1 shows the mass and proper decay time fit projections for the $B_s^0 \rightarrow J/\psi\phi$ sample demonstrating the good quality of the fit.

The results from the 7 TeV and 8 TeV data samples are consistent and are combined:

$$\phi_s = (-0.098 \pm 0.084 \text{ (stat.)} \pm 0.040 \text{ (syst.)}) \text{ rad}, \quad (2.8)$$

$$\Delta\Gamma_s = (0.083 \pm 0.011 \text{ (stat.)} \pm 0.007 \text{ (syst.)}) \text{ ps}^{-1}. \quad (2.9)$$

Figure 2 shows the likelihood contours in the $\phi_s - \Delta\Gamma_s$ plane for the 7 TeV and 8 TeV analyses, separately and combined. The results agree well with the Standard Model prediction.

3. Measurement of the relative width difference of the $B^0 - \bar{B}^0$ system

A more recent heavy-flavour result [6] from ATLAS is the measurement of one of the parameters describing the time evolution of the B^0 system, $\Delta\Gamma_d$. The relative value of the $B^0 - \bar{B}^0$ width difference $\Delta\Gamma_d/\Gamma_d$ is reliably predicted [3] in the Standard Model:

$$\Delta\Gamma_d/\Gamma_d = (0.42 \pm 0.08) \times 10^{-2}. \quad (3.1)$$

It has been shown [7] that a relatively large variation of $\Delta\Gamma_d/\Gamma_d$ due to a possible new physics contribution would not contradict other existing SM results. A precise measurement of $\Delta\Gamma_d/\Gamma_d$ would therefore provide a stringent test of the underlying theory, complementary to other searches.

The current experimental uncertainty of $\Delta\Gamma_d/\Gamma_d$ is much larger than the SM central value, which prevents a meaningful test of the SM prediction. Furthermore, the measurements of $\Delta\Gamma_d/\Gamma_d$

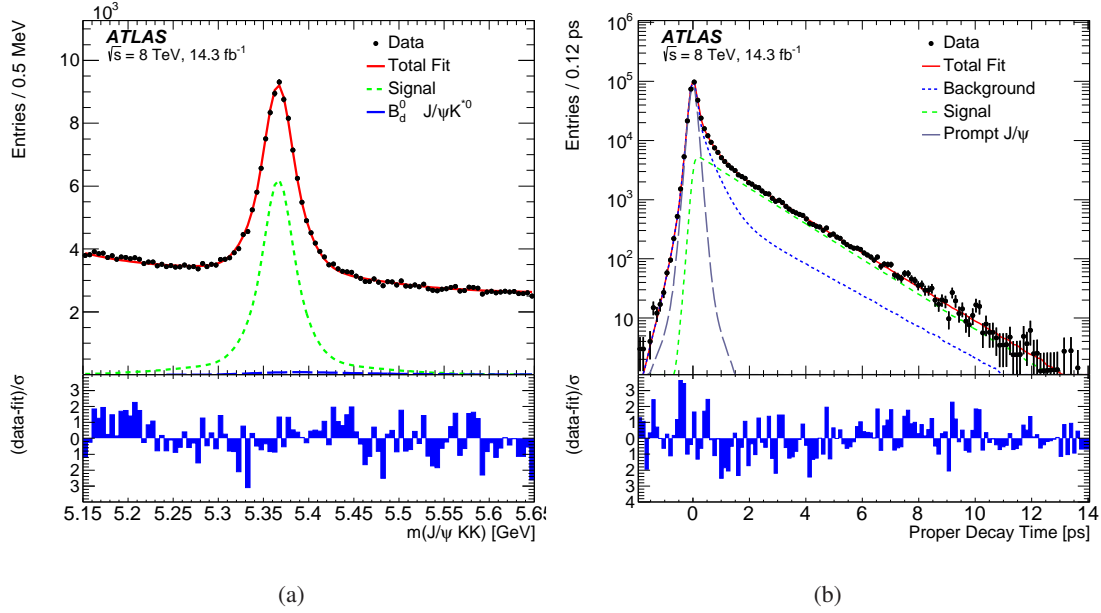


Figure 1: (a) Mass fit projection for the $B_s^0 \rightarrow J/\psi\phi$ sample. The red line shows the total fit, the dashed green line shows the signal component while the long-dashed blue line shows the contribution from $B_s^0 \rightarrow J/\psi K^{0*}$ events. (b) Proper decay time fit projection for the $B_s^0 \rightarrow J/\psi\phi$ sample. The red line shows the total fit while the green dashed line shows the total signal. The total background is shown as a blue dashed line with a long-dashed grey line showing the prompt J/ψ background. Below each figure is a ratio plot that shows the difference between each data point and the total fit line divided by the statistical uncertainty (σ) of that point; taken from [5].

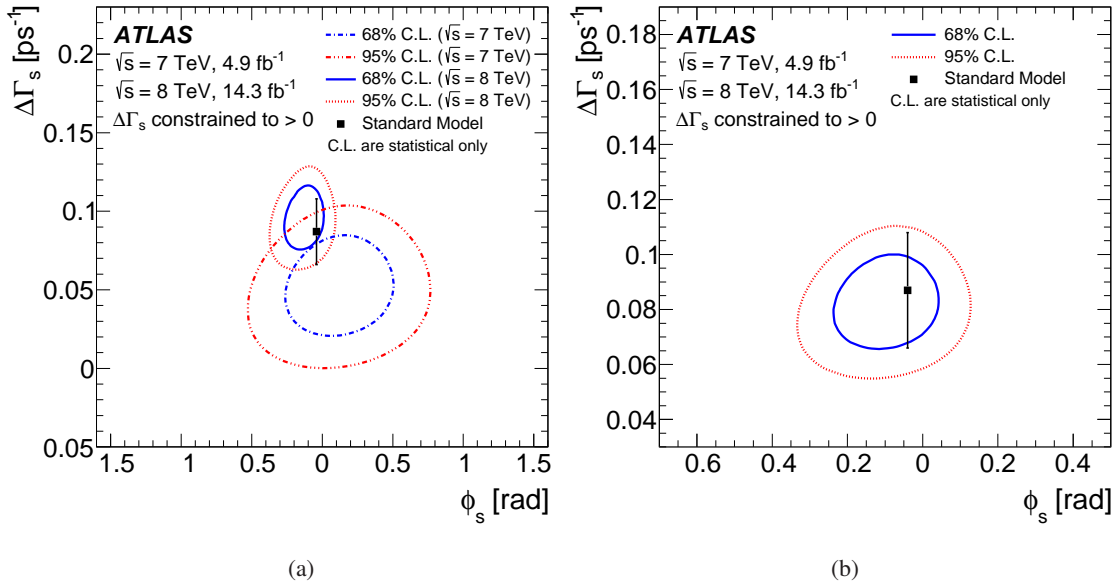


Figure 2: Likelihood contours in the $\phi_s - \Delta\Gamma_s$ plane for (a) the separate results and (b) the combined results from the $\sqrt{s} = 7$ TeV and $\sqrt{s} = 8$ TeV analyses [5]. The blue line shows the 68% likelihood contour, while the red dotted line shows the 95% likelihood contour (statistical errors only).

made by Belle [8] and LHCb [9] differ by more than 1.5 standard deviations. Therefore, more precise measurements of $\Delta\Gamma_d/\Gamma_d$ are needed to constrain this quantity and verify or disprove the SM prediction. The measurement of $\Delta\Gamma_d/\Gamma_d$ was performed by the ATLAS collaboration using the method described below.

The value of $\Delta\Gamma_d/\Gamma_d$ is determined by measuring the experimental ratio of the proper decay time (t) distributions of $B^0 \rightarrow J/\psi K_S$ and $B^0 \rightarrow J/\psi K^{*0}$ decays. The J/ψ is reconstructed using the decay $J/\psi \rightarrow \mu^+\mu^-$. The K_S and K^{*0} are reconstructed using the $K_S \rightarrow \pi^+\pi^-$ and $K^{*0} \rightarrow K^+\pi^-$ decay modes. The $B^0 \rightarrow J/\psi K^{*0}$ and $\bar{B}^0 \rightarrow J/\psi \bar{K}^{*0}$ decays are added together.

The decay time distribution of $B^0 \rightarrow J/\psi K_S$ depends on $\Delta\Gamma_d$:

$$\Gamma[t, J/\psi K_S] \propto e^{-\Gamma_d t} \left[\cosh \frac{\Delta\Gamma_d t}{2} + \cos(2\beta) \sinh \frac{\Delta\Gamma_d t}{2} - A_P \sin(2\beta) \sin(\Delta m_d t) \right], \quad (3.2)$$

while the decay time distribution of $B^0 \rightarrow J/\psi K^{*0}$ is almost insensitive to $\Delta\Gamma_d$:

$$\Gamma[t, J/\psi K^{*0}] \propto e^{-\Gamma_d t} \cosh \frac{\Delta\Gamma_d t}{2}. \quad (3.3)$$

Here Δm_d is the mass difference of the $B^0 - \bar{B}^0$ system, β is the CKM unitarity triangle angle, $\sin 2\beta = 0.679 \pm 0.020$ [10], and A_P is the production asymmetry of B^0 and \bar{B}^0 . The cancellation of the $e^{-\Gamma_d t}$ factor in the ratio of the two decay modes leads to increased sensitivity to $\Delta\Gamma_d$. Using a ratio also helps to reduce the systematic uncertainties of the measurement. The reconstruction of the two channels is designed to be similar for the same reason. Both decay modes are triggered by the same di-muon triggers and the additional particles from the B^0 decay are not used in the trigger or the proper decay time determination.

The proper decay length, $L_{\text{prop}}^B = ct$, is used for the measurement:

$$L_{\text{prop}}^B = \frac{(x^{J/\psi} - x^{\text{PV}}) + (y^{J/\psi} - y^{\text{PV}})}{(p_T^B)^2} m_{B^0}. \quad (3.4)$$

The origin of the B^0 , $(x^{\text{PV}}, y^{\text{PV}})$, is measured using a primary vertex fit in which the decay products of the B^0 are removed. The position of the B^0 decay is defined by the J/ψ decay vertex, $(x^{J/\psi}, y^{J/\psi})$, the world average [10] is used for the B^0 mass, m_{B^0} .

The decay rates $\Gamma[L_{\text{prop}}^B, f]$, $f = (J/\psi K_S, J/\psi K^{*0})$, expressed as functions of L_{prop}^B are:

$$\Gamma[L_{\text{prop}}^B, f] = \int_0^\infty G(L_{\text{prop}}^B - ct, f) \Gamma[t, f] dt, \quad (3.5)$$

where $G(L_{\text{prop}}^B - ct, f)$ is the L_{prop}^B detector resolution function for the decay mode f .

The proper decay length distribution is obtained by first dividing the range of L_{prop}^B into ten bins between -0.3 and 6.0 mm. In each L_{prop}^B bin distributions of the invariant mass of the $J/\psi K_S$ and $J/\psi K^{*0}$ candidates are produced and the number of signal $B^0 \rightarrow J/\psi K_S$ and $B^0 \rightarrow J/\psi K^{*0}$ candidates determined by a fit to these distributions. Figure 3 shows the invariant mass distributions of the $B^0 \rightarrow J/\psi K_S$ and $B^0 \rightarrow J/\psi K^{*0}$ candidates in the range $0.0 < L_{\text{prop}}^B < 0.3$ mm. The total number of $B^0 \rightarrow J/\psi K_S$ decays is $28\,170 \pm 250$ in the 7 TeV data sample and $110\,830 \pm 520$ in the 8 TeV data sample. For $B^0 \rightarrow J/\psi K^{*0}$ decays, the total number of candidates is $129\,200 \pm 900$ in the 7 TeV data sample and $555\,800 \pm 1\,900$ in the 8 TeV sample.

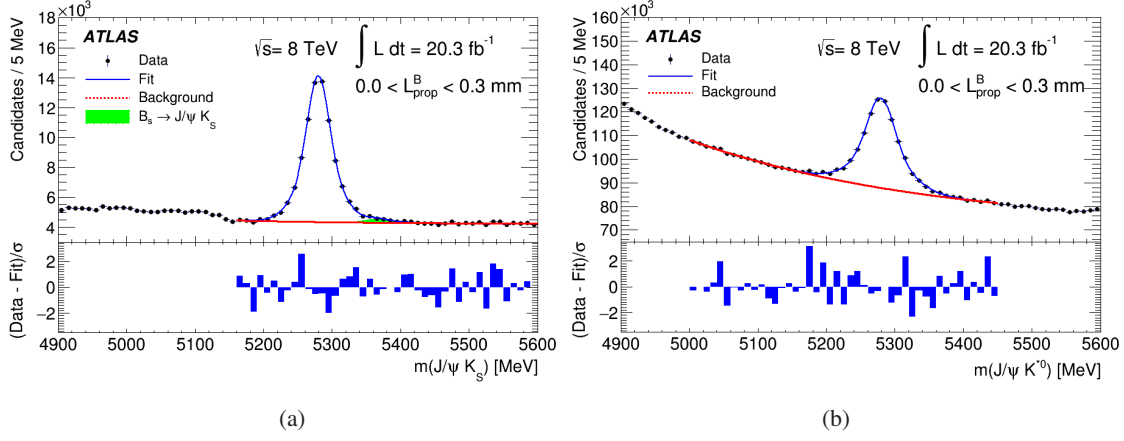


Figure 3: The invariant mass distributions for (a) $B^0 \rightarrow J/\psi K_S$ candidates and (b) $B^0 \rightarrow J/\psi K^{*0}$ candidates for the 2012 data sample for $0.0 < L_{\text{prop}}^B < 0.3$ mm. The full line shows the result of the fit to the function described in [6]. The dashed line shows the combinatorial background contribution. The filled area in figure (a) shows the peaking background contribution from the $B_s \rightarrow J/\psi K_S$ decay. The lower frame of each figure shows the difference between each data point and the fit at that point divided by the statistical uncertainty of the data point.

The ratio of the number of B^0 candidates in the two channels in each L_{prop}^B bin gives the experimental ratio $R_{i,\text{uncor}}(L_{\text{prop}}^B)$. This ratio is corrected to account for the difference in reconstruction efficiencies of the $B^0 \rightarrow J/\psi K_S$ and $B^0 \rightarrow J/\psi K^{*0}$ channels. This difference is mainly due to the fact that the hadronic tracks in the $B^0 \rightarrow J/\psi K_S$ decay come from a displaced $K_S \rightarrow \pi\pi$ vertex, while all four tracks from the $B^0 \rightarrow J/\psi K^{*0}$ decay come from a single vertex. This is the largest source of experimental bias in $R_{i,\text{uncor}}(L_{\text{prop}}^B)$ and it can be assessed only with Monte Carlo (MC) simulation. The ratio of reconstruction efficiencies in MC is determined in each L_{prop}^B bin and used to obtain the corrected ratio $R_{i,\text{cor}}(L_{\text{prop}}^B)$, from which the value of $\Delta\Gamma_d/\Gamma_d$ can be extracted.

The $B^0 - \bar{B}^0$ production asymmetry in ATLAS is measured from the charge asymmetry of the $B^0 \rightarrow J/\psi K^{*0}$ decay, which is measured as a function of L_{prop}^B . The charge asymmetry has two contributions: the detector asymmetry A_{det} and the production asymmetry A_P . The latter should oscillate with L_{prop}^B . The distribution of A_{obs} is shown in Fig. 4. The offset from 0 is due to the detector asymmetry A_{det} .

The value of A_P measured by the ATLAS experiment using data obtained at 7 and 8 TeV is:

$$A_P = (+0.25 \pm 0.48 \text{ (stat.)} \pm 0.05 \text{ (syst.)}) \times 10^{-2}. \quad (3.6)$$

The relative width difference $\Delta\Gamma_d/\Gamma_d$ is obtained from a χ^2 minimisation:

$$\chi^2 [\Delta\Gamma_d/\Gamma_d] = \sum_{i=2}^{10} \frac{(R_{i,\text{cor}} - R_{i,\text{exp}} [\Delta\Gamma_d/\Gamma_d])^2}{\sigma_i^2}, \quad (3.7)$$

where $R_{i,\text{exp}}$ is the expected ratio of the decay rates in the two channels in L_{prop}^B bin i . The fitted distributions of $R_{i,\text{cor}}(L_{\text{prop}}^B)$ for the 7 and 8 TeV data samples are shown in Fig. 5. The values of $\Delta\Gamma_d/\Gamma_d$ are obtained separately for the $\sqrt{s} = 7$ TeV and $\sqrt{s} = 8$ TeV data samples:

$$\Delta\Gamma_d/\Gamma_d = (-2.8 \pm 2.2 \text{ (stat.)} \pm 1.7 \text{ (syst.)}) \times 10^{-2} \quad [\sqrt{s} = 7 \text{ TeV}], \quad (3.8)$$

$$\Delta\Gamma_d/\Gamma_d = (+0.8 \pm 1.3 \text{ (stat.)} \pm 0.8 \text{ (syst.)}) \times 10^{-2} \quad [\sqrt{s} = 8 \text{ TeV}]. \quad (3.9)$$

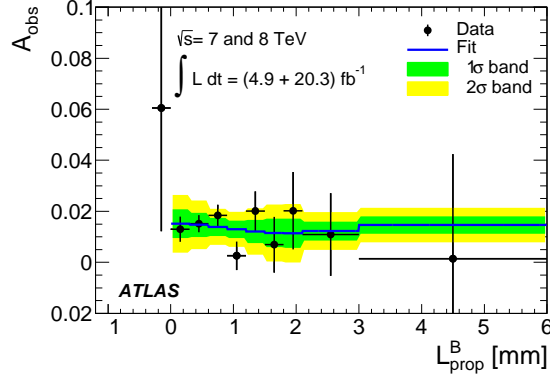


Figure 4: Observed charge asymmetry A_{obs} in $B^0 \rightarrow J/\psi K^{*0}$ decays measured as a function of the proper decay length of the B^0 meson (L_{prop}^B) [6]. The line shows the fit to the distribution by a function combining A_{det} and A_P . The first point corresponding to negative proper decay length is not used in the fit. The error bands correspond to the combination of uncertainties obtained by the fit for A_{det} and A_P .

The results from the two data samples are consistent and are combined:

$$\Delta\Gamma_d/\Gamma_d = (-0.1 \pm 1.1 \text{ (stat.)} \pm 0.9 \text{ (syst.)}) \times 10^{-2}. \quad (3.10)$$

This is currently the most precise single measurement of $\Delta\Gamma_d/\Gamma_d$. The result agrees with the SM prediction. It is also consistent with measurements performed by other experiments.

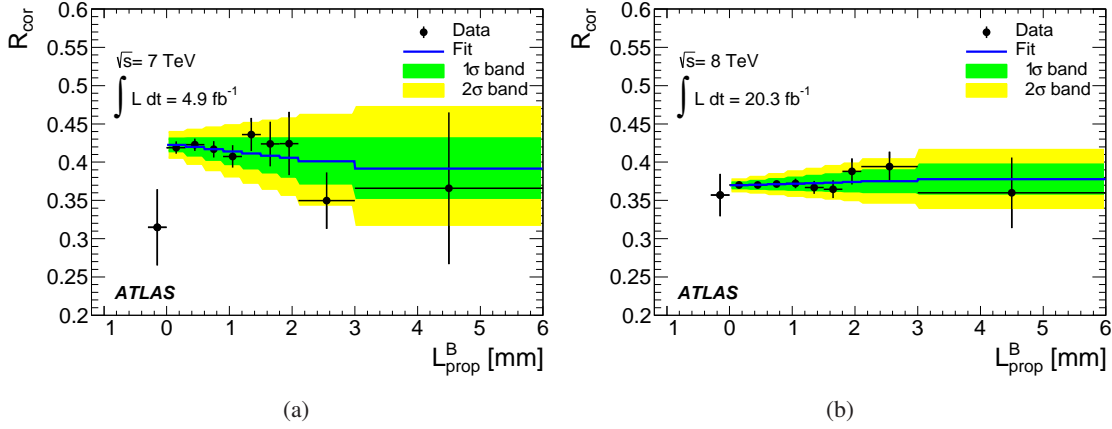


Figure 5: Efficiency-corrected ratio of the observed decay length distributions, $R_{\text{cor}}(L_{\text{prop}}^B)$ for the (a) $\sqrt{s} = 7$ TeV and (b) $\sqrt{s} = 8$ TeV data samples [6]. The normalisation of the two data sets is arbitrary. The full line shows the fit of $R_{\text{cor}}(L_{\text{prop}}^B)$. The error bands correspond to uncertainties in $\Delta\Gamma_d/\Gamma_d$ determined by the fit.

4. Conclusions

The analysis of the data collected by the ATLAS experiment during Run 1 of the LHC has revealed no anomalies in the $B_s^0 \rightarrow J/\psi\phi$ decay mode. The measurement of the CP violating weak phase ϕ_s agrees with the SM prediction and is consistent with measurements by other experiments. There is, however, still room for new physics in CP violation in this channel.

The value of $\Delta\Gamma_d/\Gamma_d$ obtained by ATLAS during Run 1 of the LHC is currently the most precise measurement of this quantity. The result agrees with the SM prediction. It is also consistent with measurements performed by other experiments.

The LHC Run-2 data should allow the precision of these measurements to be considerably improved, leading to further tests of the Standard Model validity.

References

- [1] ATLAS Collaboration, *The ATLAS Experiment at the CERN Large Hadron Collider*, *JINST* **3** (2008) S08003.
- [2] J. Charles *et al.*, *Predictions of selected flavor observables within the standard model*, *Phys. Rev. D* **84** (2011) 033005.
- [3] A. Lenz and U. Nierste, *Numerical Updates of Lifetimes and Mixing Parameters of B Mesons*, arXiv:1102.4274 [hep-ph].
- [4] ATLAS Collaboration, *Flavor tagged time-dependent angular analysis of the $B_s \rightarrow J/\psi\phi$ decay and extraction of $\Delta\Gamma_s$ and the weak phase ϕ_s in ATLAS*, *Phys. Rev. D* **90** (2014), 052007.
- [5] ATLAS Collaboration, *Measurement of the CP-violating phase ϕ_s and the B_s^0 meson decay width difference with $B_s^0 \rightarrow J/\psi\phi$ decays in ATLAS*, *JHEP* **1608** (2016) 147.
- [6] ATLAS Collaboration, *Measurement of the relative width difference of the B^0 - \bar{B}^0 system with the ATLAS detector*, *JHEP* **1606** (2016) 081.
- [7] C. Bobeth, U. Haisch, A. Lenz, B. Pecjak and G. Tetlalmatzi-Xolocotzi, *On new physics in $\Delta\Gamma_d$* , *JHEP* **1406** (2014) 040.
- [8] T. Higuchi *et al.* [Belle Collaboration], *Search for Time-Dependent CPT Violation in Hadronic and Semileptonic B Decays*, *Phys. Rev. D* **85** (2012) 071105.
- [9] R. Aaij *et al.* [LHCb Collaboration], *Measurements of the B^+ , B^0 , B_s^0 meson and Λ_b^0 baryon lifetimes*, *JHEP* **1404** (2014) 114.
- [10] K.A. Olive and Particle Data Group, *Review of Particle Physics*, *Chin. Phys. C* **38(9)** (2014) 090001.